

CSI-Free Position Optimization for Movable Antenna Communication Systems: A Black-Box Optimization Approach

Xianlong Zeng, Jun Fang, Bin Wang, Boyu Ning, and Hongbin Li, *Fellow, IEEE*

Abstract—Movable antenna (MA) is a new technology which leverages local movement of antennas to improve channel qualities and enhance the communication performance. Nevertheless, to fully realize the potential of MA systems, complete channel state information (CSI) between the transmitter-MA and the receiver-MA is required, which involves estimating a large number of channel parameters and incurs an excessive amount of training overhead. To address this challenge, in this paper, we propose a CSI-free MA position optimization method. The basic idea is to treat position optimization as a black-box optimization problem and calculate the gradient of the unknown objective function using zeroth-order (ZO) gradient approximation techniques. Simulation results show that the proposed ZO-based method, through adaptively adjusting the position of the MA, can achieve a favorable signal-to-noise-ratio (SNR) using a smaller number of position measurements than the CSI-based approach. Such a merit makes the proposed algorithm more adaptable to fast-changing propagation channels.

Index terms— Movable antenna, CSI-free, position optimization.

I. INTRODUCTION

Movable antenna (MA) is a new technology that allows antennas movable over a specified region to obtain a better channel quality [1]–[3]. With the aid of mechanical controllers and drivers, MA can provide additional degrees of freedom (DoF) and achieve significant communication gains [2]. While this additional spatial DoF can also be utilized by antenna selection (AS) technologies in MIMO communication systems [4], [5], this approach requires deployment of a large number of antennas to cover the spatial region, thus resulting in an increased hardware cost. In contrast, MA is able to fully exploit the spatial DoFs with much fewer antennas or even a single antenna.

Over the past few years, many efforts have been made to investigate the potential of the MA systems, e.g. [3], [6]–[8]. In [3], it was shown that jointly optimizing the positions of the receive and transmit MAs can improve the spatial multiplexing performance of MIMO systems. The MA-aided interference suppression problem was investigated in [7], which showed that MA-assist multiuser systems can not only increase the receive signal power, but also achieve effective interference

mitigation. In addition, the work [8] discussed general architectures and implementation methods for realizing MA in existing communication systems.

Despite the advantages of MA systems over fixed-position antenna (FPA) systems, the operation of the MA system relies on the complete knowledge of the channel response between the transmitter (Tx) and the receiver (Rx) over the entire movable regions [9]. If channel measurement is taken for every point over the movable region in order to find a best MA position, this would undoubtedly involve an excessive amount of time and training overhead. To address this issue, a compressed sensing-based method was proposed in [10] by exploiting the multi-path field response channel structure. Based on multiple measurements taken at designated positions of the Tx-MA and Rx-MA, the channel parameters associated with multi-path components can be estimated via a compressed sensing approach and the channel response over the entire movable regions can be reconstructed. Such a compressed sensing-based approach, however, faces difficulties under rich-scattering channels with a large number of multi-path components.

In this paper, we propose a CSI-free position optimization approach for MA-assisted communication systems. The idea is to treat position optimization as a black-box optimization problem, and estimate the gradient of the objective function via zeroth-order (ZO) gradient approximation methods. Specifically, based on the received signals collected from previous positions, the receiver calculates a new position and the MA is then moved to this new position to take measurements for next position refinement. Such a procedure is repeated until a convergence is reached. Simulation results show that the proposed method is more sample-efficient than the CSI-based method in optimizing the MA's position. Moreover, another advantage of our proposed approach it only utilizes the magnitude of the received signals for position optimization, which enhances the algorithm's robustness against phase noise/errors inevitably present in the receiver system.

II. SYSTEM MODEL

We consider a movable antenna (MA)-aided point-to-point narrowband communication system, where a single MA is employed at the receiver, and a single fixed-position antenna is employed at the transmitter. Such a simple system model helps facilitate the exposition of the idea of our work. Our proposed scheme can also be extended to the joint TX-RX

Xianlong Zeng, Jun Fang, Bin Wang and Boyu Ning are with the National Key Laboratory of Wireless Communications, University of Electronic Science and Technology of China, Chengdu 611731, China, Emails: Jun-Fang@uestc.edu.cn; boyuning@outlook.com

Hongbin Li is with the Department of Electrical and Computer Engineering, Stevens Institute of Technology, Hoboken, NJ 07030, USA, Email: Hongbin.Li@stevens.edu

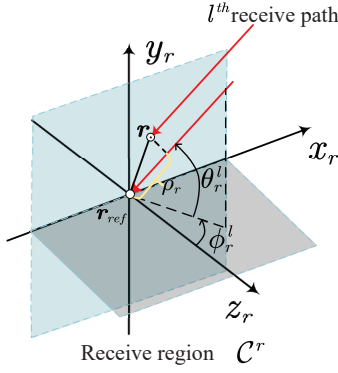


Fig. 1: Schematic of Rx-MA's coordinates and geometric relationships

MA system at the cost of involving additional feedback from the RX to the TX.

As illustrated in Fig. 1, we establish a local Cartesian coordinate system to describe the position of the receive antenna. The position of the RX's antenna is denoted as $\mathbf{r} = [x^r, y^r] \in \mathcal{C}^r$, where \mathcal{C}^r is a two-dimensional square region of size $A \times A$ in which the antenna can be flexibly positioned.

Denoting the channel from the Tx to the Rx as $h(\mathbf{r})$, the received signal at the Rx can be expressed as

$$y(\mathbf{r}) = \sqrt{P}h(\mathbf{r})s + n, \quad (1)$$

where s denotes the transmitted signal, P is the transmit power and n denotes the additive white Gaussian noise with zero mean and variance σ^2 .

Note that the channel response h between the TX and the RX is a superposition of multi-path components (MPCs). Specifically, it can be modeled by the geometric channel model as

$$h = \sum_{l=1}^L b_l = \sum_{l=1}^L \alpha_l e^{j\delta_l}, \quad (2)$$

where $b_l \triangleq \alpha_l e^{j\delta_l}$ represents the complex coefficient associated with the l th path, α_l and δ_l respectively represent the magnitude and the phase of b_l . The above channel response model, however, does not take the position of the antenna into account. To model the effect of the MA's position, we first consider (2) as the channel response from the TX to the receive reference position $\mathbf{r}_{ref} = [0, 0]^T$, and express h as

$$h(\mathbf{r}_{ref}) = \mathbf{1}_L^H \mathbf{\Gamma}, \quad (3)$$

where $\mathbf{\Gamma} \triangleq [b_1 \ b_2 \ \dots \ b_L]^T = [\alpha_1 e^{j\delta_1} \ \dots \ \alpha_L e^{j\delta_L}]^T \in \mathbb{C}^L$ denotes the path response vector and $\mathbf{1}_L \in \mathbb{R}^L$ denotes a vector with all entries equal to one.

Here, we assume that the far-field condition is satisfied between the TX and the RX, where the size of \mathcal{C}^r is much smaller than the propagation distance. Hence, the angles of arrival (AoAs) and the complex coefficients of MPCs are approximately the same over the region \mathcal{C}^r . Nevertheless, as the antenna moves from the reference point $[0, 0]$ to position $[x_r, y_r]$, the signal propagation time of each path changes,

which in turn results in a phase variation. Specifically, as illustrated in Fig. 1, denote θ_r^l and ϕ_r^l as the l -th path's elevation AoA and azimuth AoA, respectively. When the RX-MA moves to position $\mathbf{r} = [x_r, y_r]$ from $\mathbf{r}_{ref} = [0, 0]$, the signal propagation distance for the l -th path is changed by

$$\rho_r^l(x_r, y_r) = x_r \cos \theta_r^l \sin \phi_r^l + y_r \sin \theta_r^l, \quad (4)$$

As a result, the l -th path incurs a phase variation of $\frac{2\pi}{\lambda} \rho_r^l(x_r, y_r)$ at position $\mathbf{r} = [x_r, y_r]$ with respect to position $\mathbf{r}_{ref} = [0, 0]$, where λ denotes the wavelength of the signal. Therefore, the channel response between the TX and the RX-MA located at $\mathbf{r} = [x_r, y_r]$ can be expressed as

$$h(\mathbf{r}) = \sum_{l=1}^L b_l e^{-j\frac{2\pi}{\lambda} \rho_r^l(x_r, y_r)} = \mathbf{f}(\mathbf{r})^H \mathbf{\Gamma}, \quad (5)$$

where $\mathbf{f}(\mathbf{r}) \in \mathbb{C}^L$ denotes the receiver-side field response vector accounting for the phase variations, which is given by

$$\mathbf{f}(\mathbf{r}) = \left[e^{j\frac{2\pi}{\lambda} \rho_r^1(x_r, y_r)} \ \dots \ e^{j\frac{2\pi}{\lambda} \rho_r^L(x_r, y_r)} \right]^T.$$

We see that the channel response between the TX and the RX is dependent on the position of the Rx-MA. As a result, through changing/configuring the position of the MA, a better performance, e.g. a higher signal-to-noise ratio, can be obtained.

III. PROBLEM FORMULATION

To evaluate the performance of MA-aided communication systems, we adopt the signal-to-noise ratio (SNR) as a metric. According to (1), the SNR for the received signal is given by

$$\gamma(\mathbf{r}) = \frac{|h(\mathbf{r})|^2 P}{\sigma^2}. \quad (6)$$

Here the SNR is depended on the position of the RX-MA.

Our objective is to maximize the receive SNR via optimizing the Rx-MA position. Such a problem can be formulated as

$$\begin{aligned} \text{(P1)} \quad & \max_{\mathbf{r}} \gamma(\mathbf{r}) = \frac{|h(\mathbf{r})|^2 P}{\sigma^2} \\ & \text{s.t.} \quad \mathbf{r} \in \mathcal{C}^r. \end{aligned} \quad (7)$$

Since the transmit power P and the noise power σ^2 are constants, problem (P1) is equivalent to maximizing $|h(\mathbf{r})|^2$, which is further expressed as

$$\begin{aligned} |h(\mathbf{r})|^2 &= \left| \sum_{l=1}^L b_l e^{-j\frac{2\pi}{\lambda} \rho_r^l(x_r, y_r)} \right|^2 \\ &= \sum_{m=1}^L \sum_{n=1}^L |\alpha_m| |\alpha_n| \cos \left(\frac{2\pi}{\lambda} \varrho_{mn} + c_{mn} \right). \end{aligned} \quad (8)$$

where $\varrho_{mn}(\mathbf{r}) \triangleq \rho_r^m(x_r, y_r) - \rho_r^n(x_r, y_r)$ and $c_{mn} \triangleq \delta_n - \delta_m$.

From (8), we see that the optimization of the MA's position requires the knowledge of the channel parameters $\{b_l, \theta_r^l, \phi_r^l\}_{l=1}^L$. To obtain these channel parameters, we need to measure the channel $h(\mathbf{r})$ at different positions, say, $\{\mathbf{r}_m\}_{m=1}^M$, and collect the measured channel samples $\{h(\mathbf{r}_m)\}_{m=1}^M$. Based on the measured channel samples

$\{h(\mathbf{r}_m)\}_{m=1}^M$, the channel parameters $\{b_l, \theta_r^l, \phi_r^l\}_{l=1}^L$ can be estimated via compressed sensing or other signal processing techniques. Such a channel estimation-based approach, however, may require an excessively large number of channel measurements for rich scattering scenarios consisting of a heavy number of MPCs.

To overcome the drawback of existing approaches, in this paper we propose a CSI-free approach which does not need the knowledge of the channel parameters for position optimization.

IV. PROPOSED METHOD

Note that the objective function of (7) has unknown channel parameters, making it challenging or even impossible to compute explicit expressions of its gradient. Such optimization problems involving unknown objective functions are known as block-box optimization problems, and have been investigated by many prior works. Although there are different approaches (such as Bayesian optimization [11], derivative-free trust region methods [12], and genetic algorithms [13]) to address the block-box optimization problem. Among them, the zeroth-order (ZO) optimization method [14]–[16] has gained an increasing attention due to its unique advantages: first, ZO methods are easy to implement as they are based on commonly used gradient-based algorithms; second, ZO methods can achieve comparable convergence rates to first-order algorithms.

A. ZO Optimization Method

The basic idea of ZO optimization is to approximate the full gradients or stochastic gradients through function value-based gradient estimates. Specifically, for an unknown function f , the ZO gradient is estimated as the central difference of two function values at a random unit direction [15]:

$$\hat{\nabla} f(\mathbf{x}) = (d/2\mu)[f(\mathbf{x} + \mu\mathbf{u}) - f(\mathbf{x} - \mu\mathbf{u})]\mathbf{u} \quad (9)$$

where \mathbf{u} is a random vector drawn from the sphere of a unit ball, μ is a small step size and d denotes a dimension-dependent factor. In some cases, \mathbf{u} can be also randomly chosen as a standard unit vector \mathbf{e}_i with 1 at its i th coordinate and zeros elsewhere.

Most ZO optimization methods mimic their first-order counterparts and involve three steps, namely, gradient estimation, descent direction computation, and point updating. The gradient estimation can be performed using (9). For different ZO methods, their major difference lies in the strategies used to form the descent direction. Note that the estimated gradient (9) is stochastic in nature and may suffer from a large estimation variance, which causes poor convergence performance. To address this issue, different descent direction update schemes were proposed. Among them, the ZO-AdaMM [14] has been proven to be an effective method that is robust against gradient estimation errors and achieves a superior convergence speed. Due to its simplicity and superior performance, here we adopt ZO-AdaMM to solve our position optimization problem.

For clarity, we provide a summary of ZO-AdaMM in Algorithm 1.

Algorithm 1 ZO-AdaMM

Require: step size α , hyper-parameters $\beta_1, \beta_2 \in (0, 1]$, and set $\mathbf{m}_0, \mathbf{v}_0$

- 1: Initialize the MA position \mathbf{r}_0 .
- 2: **while** not converge **do**
- 3: $t \leftarrow t + 1$
- 4: Estimate $\tilde{\mathbf{g}}_t = \hat{\nabla} f(\mathbf{x})$ according to (9)
- 5: let $\mathbf{m}_t = \beta_1 \mathbf{m}_{t-1} + (1 - \beta_1) \tilde{\mathbf{g}}_t$
- 6: $\mathbf{v}_t = \beta_2 \mathbf{v}_{t-1} + (1 - \beta_2) \tilde{\mathbf{g}}_t \circ \tilde{\mathbf{g}}_t$
- 7: $\hat{\mathbf{m}}_t = \frac{\mathbf{m}_t}{1 - \beta_1^t}$
- 8: $\hat{\mathbf{v}}_t = \frac{\mathbf{v}_t}{1 - \beta_2^t}$, and $\hat{\mathbf{V}}_t = \text{diag}(\hat{\mathbf{v}}_t)$
- 9: Update $\mathbf{r}_{t+1} \leftarrow \mathbf{r}_t + \alpha \hat{\mathbf{V}}_t^{-\frac{1}{2}} \hat{\mathbf{m}}_t$
- 10: **end while**

Ensure: \mathbf{r}^*

In summary, the ZO-AdaMM is a stochastic gradient descent method that consists of three steps, namely, estimation of the ZO gradient, descent direction and learning rate calculation, and variable (i.e. position) update.

First, for each position \mathbf{r} , the ZO-AdaMM employs (9) to compute an estimate of the ZO gradient:

$$\begin{aligned} \tilde{\mathbf{g}} &= \hat{\nabla} f(\mathbf{x}) \approx \frac{d(\gamma(\mathbf{r} + \mu\mathbf{u}) - \gamma(\mathbf{r} - \mu\mathbf{u}))}{2\mu} \mathbf{u} \\ &\stackrel{(a)}{=} \frac{d \left(|h(\mathbf{r} + \mu\mathbf{u})|^2 - |h(\mathbf{r} - \mu\mathbf{u})|^2 \right)}{2\mu} \mathbf{u} \quad (10) \\ &\approx \frac{d \left(|y(\mathbf{r} + \mu\mathbf{u})|^2 - |y(\mathbf{r} - \mu\mathbf{u})|^2 \right)}{2\mu} \mathbf{u} \end{aligned}$$

where $\tilde{\mathbf{g}}$ denotes the estimated gradient vector, and in (a), we ignore the scaling term P/σ^2 as it is independent of the optimization variable. In our algorithm, the vector \mathbf{u} is randomly chosen as a standard unit vector for each iteration. Note that, since the channel $h(\mathbf{r})$ is not directly available, we use its noisy version $y(\mathbf{r})$ (cf. (1)) to calculate the gradient. On the other hand, the gradient estimate $\tilde{\mathbf{g}}$ becomes more accurate when a smaller μ is adopted. However, if μ is set too small, the function difference could be dominated by the noise and thus yields a poor gradient estimate. Thus, a proper choice of the parameter μ is important for the convergence of ZO-AdaMM.

In the second step of ZO-AdaMM, we need to calculate the descent direction and the adaptive learning rate. The descent direction is given by an exponential moving average of past gradients. Specifically, at each iteration, the descent direction can be updated as

$$\mathbf{m}_t = \beta_1 \mathbf{m}_{t-1} + (1 - \beta_1) \tilde{\mathbf{g}}_t \quad (11)$$

where the hyperparameter $\beta_1 \in [0, 1)$ controls the exponential decay rate of the moving averages. In particular, the descent direction is not only determined by the gradient at the current iteration, but also depends on past gradients. The second moment vector is adaptively calculated as

$$\mathbf{v}_t = \beta_2 \mathbf{v}_{t-1} + (1 - \beta_2) \tilde{\mathbf{g}}_t \circ \tilde{\mathbf{g}}_t \quad (12)$$

where the hyperparameter $\beta_2 \in [0, 1)$ controls the exponential decay rate of the moving averages and \circ denotes the Hadamard product.

Typically, \mathbf{m}_0 and \mathbf{v}_0 are initialized as zeros. This results in moving averages \mathbf{m}_t and \mathbf{v}_t that are biased towards zero, especially during the initial few iterations. This bias can be easily counteracted, by adopting bias-corrected estimates $\hat{\mathbf{m}}_t, \hat{\mathbf{v}}_t$, i.e.,

$$\hat{\mathbf{m}}_t = \frac{\mathbf{m}_t}{1 - \beta_1^t} \quad (13)$$

$$\hat{\mathbf{v}}_t = \frac{\mathbf{v}_t}{1 - \beta_2^t} \quad (14)$$

At the beginning, the values of \mathbf{m}_t and \mathbf{v}_t are small because they are weighted averages of estimated gradients, and the initial values are set as 0. Nevertheless, we can amplify the \mathbf{m}_t and \mathbf{v}_t by the bias correction factor $\{1 - \beta_i^t, i = 1, 2\}$ to make them closer to the actual moving averages. In particular, as the number of iterations increases, the value of β_i^t converges to 0 and the bias correction factor will finally approach to 1, so that the effect of the bias correction will gradually diminish.

After the descent direction and the second moment vector are calculated, the MA position can be updated as

$$\mathbf{r}_{t+1} \leftarrow \mathbf{r}_t + \alpha \hat{\mathbf{V}}_t^{-\frac{1}{2}} \hat{\mathbf{m}}_t \quad (15)$$

where $\hat{\mathbf{V}}_t \triangleq \text{diag}\{\hat{\mathbf{v}}_t\}$ and α denotes the step size. $\alpha \hat{\mathbf{V}}_t^{-\frac{1}{2}}$ can be interpreted as the adaptive learning rate which can dynamically adjust the step size. Particular, when the slope is steeper, the step size will become smaller to avoid missing the optimal point, which ensures the robustness of the algorithm. From another perspective, the rationale behind the above equation is to normalize the estimated descent direction to reduce the noise effect. We can see that ZO-AdaMM normalizes the descent direction $\hat{\mathbf{m}}_t$ by $\sqrt{\hat{\mathbf{v}}_t}$. In particular, $\hat{\mathbf{m}}_t/\sqrt{\hat{\mathbf{v}}_t}$ is invariant to the scale of the gradients. Scaling the gradient with factor c will scale $\hat{\mathbf{m}}_t$ with a factor c and $\hat{\mathbf{v}}_t$ with a factor c^2 , which cancel out this scaling factor as we have $c\hat{\mathbf{m}}_t/\sqrt{c^2\hat{\mathbf{v}}_t} = \hat{\mathbf{m}}_t/\sqrt{\hat{\mathbf{v}}_t}$.

B. Other Implementing Issues

A good initialization point can help the ZO-AdaMM algorithm converge to the desired minimum more quickly. To obtain a good initialization point, we can have the RX-MA move to different positions to measure the channel magnitude and select the position with the largest magnitude. Specifically, we randomly pick a set of candidate positions defined as $\mathcal{R}^{ini} = \{\mathbf{r}_1^{ini}, \dots, \mathbf{r}_N^{ini}\}$. The corresponding measurements of these candidate locations are given as $\mathcal{Y}^{ini} = \{|y(\mathbf{r}_1^{ini})|, \dots, |y(\mathbf{r}_N^{ini})|\}$. Let $S_{ini} \triangleq \{n | |y(\mathbf{r}_n^{ini})| \geq |y(\mathbf{r}_i^{ini})|, \forall i = 1, \dots, N\}$ denote the index of the largest element in \mathcal{Y}^{ini} . Then the initial position can be set to $\mathbf{r}_0 = \mathbf{r}_{S_{ini}^{ini}}$.

Another issue is that the algorithm may produce a position that is out of the feasible region. In this case, we project its position component to the corresponding edge value, i.e.,

$$[\mathbf{r}]_i = \begin{cases} -\frac{A}{2} & \text{if } [\mathbf{r}]_i < -\frac{A}{2}, \\ \frac{A}{2} & \text{if } [\mathbf{r}]_i > \frac{A}{2}, \\ [\mathbf{r}]_i & \text{otherwise.} \end{cases} \quad (16)$$

V. SIMULATION RESULT

We now presents simulation results to show the efficiency of the proposed CSI-free ZO method for position optimization. During the training stage, the TX equipped with an FPA transmits a constant signal $s = 1$ to the receiver. Based on the received signals collected from previous positions $\{y(\mathbf{r}_t \pm \mu \mathbf{u}_t)\}_{t=0}^{t'}$, the receiver calculates a new position, $\mathbf{r}_{t'+1}$, according to Algorithm 1, and then collects measurements at positions $\mathbf{r}_{t'+1} \pm \mu \mathbf{u}_{t'+1}$ for subsequent position update. This procedure is repeated until a convergence is reached. Note that here \mathbf{u}_t represents the standard unit vector randomly chosen at the t th iteration.

In our experiments, the channel is generated according to (5), where the path response coefficients $\{b_l\}$ are independent and identically distributed (i.i.d.) circularly symmetric complex Gaussian random variables, i.e., $b_l \sim \mathcal{CN}(0, 1/L)$. The elevation AoA and the azimuth AoA associated with each path are uniformly chosen over the interval $[-\pi/2, \pi/2]$. The region in which the MA can be flexibly adjusted is set to a square area with a size of $4\lambda \times 4\lambda$, i.e., $\mathcal{C}_r = [-2\lambda, 2\lambda] \times [-2\lambda, 2\lambda]$. For our proposed method, the hyper-parameters β_1 and β_2 are set respectively as $\beta_1 = 0.9$ and $\beta_2 = 0.99$. The transmit power is set to $P = 30\text{dBm}$ and the transmit signal-to-noise ratio (SNR) is set to $P/\sigma^2 = 30\text{dB}$. The performance of the proposed method is evaluated by the receive SNR (6) corresponding to the MA's position obtained by the proposed method.

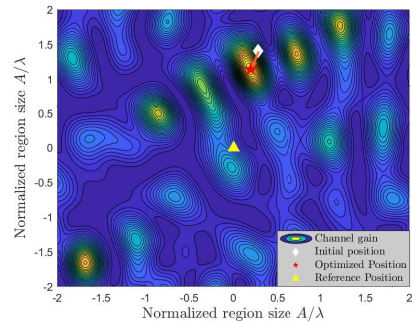


Fig. 2: Variation of the receive SNR over the movable region.

In Fig. 2, we depict the variation of the receive SNR over the entire movable region, where we set the number of paths $L = 30$. It can be seen that, due to the small-scale fading in the spatial domain, the channel quality varies drastically across the movable region. In the figure, the reference point $[0, 0]$ of the MA has a receive SNR of 11.5dB. After some iterations, the proposed algorithm finally converges to a position $[0.36\lambda, 1.01\lambda]$, which yields a receive SNR of 18.4dB,

and achieves an SNR increase of about 6.9dB as compared to the reference point.

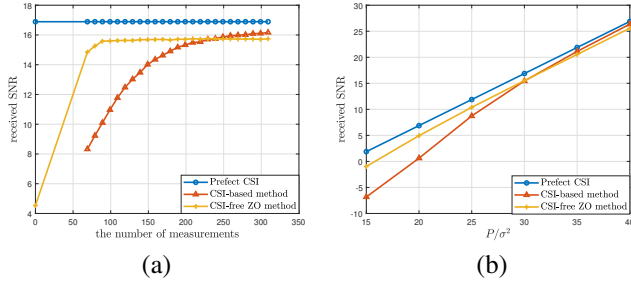


Fig. 3: (a) Receive SNRs achieved by respective methods; (b) received SNRs versus the noise variance.

Note that our proposed method requires a total number of $T' = N + 2T$ channel measurements, in which the first N measurements are used to determine a good initialization point and the rest $2T$ measurements are used to calculate the ZO gradients during the iterative process, with 2 samples needed at each iteration for computing the current ZO gradient and T being the total number of iterations performed by the algorithm. To show the sample efficiency of the proposed algorithm, we compare our CSI-free method with the CSI-based method [10]. For the CSI-based method, the MA needs to collect multiple channel measurements at designated or randomly selected positions and then use a compressed sensing-based method to estimate the channel parameters. After the channel parameters are estimated, the optimum position that achieves the maximum receive SNR can be determined via a two-dimensional search.

Fig.3(a) illustrates the receive SNRs of respective methods versus the total number of channel measurements, where the number of paths is set to $L = 30$. We see that our proposed algorithm presents a clear performance advantage over the CSI-based method in terms of sampling efficiency: it requires only about $T' = 69$ channel samples to find a good point that achieves a receive SNR close to the maximum achievable SNR, whereas the CSI-based method takes about $T' = 209$ channel samples to attain a similar performance. When the number of samples is limited, say $T' = 100$, our proposed algorithm is able to achieve a significant SNR performance advantage over the CSI-based method.

Next, we show the performance of respective methods as a function of the noise variance. Note that both our proposed method and the CSI-based method rely on the received channel measurements $y(\mathbf{r})$ to find a good position for the RX-MA. Therefore it is interesting to examine the behavior of respective algorithms when the measurements are corrupted by different amounts of noise levels. Fig. 3 (b) depicts the receive SNRs achieved by respective methods versus the noise variance, where the total number of channel measurements and the number of paths are set to $T' = 209$ and $L = 30$, respectively. We see that our proposed method exhibits a better performance than the CSI-based method when the noise level added to the measurements is high. This improved robustness against noise comes from the fact that our proposed method does not need

to explicitly acquire the channel parameters, instead, it simply uses the channel measurements to calculate an estimate of the gradient of the objective function. As the ZO-AdaMM method is robust against estimation errors of the gradients, it explains why our proposed method presents a performance improvement over the CSI-based method in a low SNR regime.

VI. CONCLUSIONS

In this paper, we proposed a CSI-free position optimization approach for MA-assisted communication systems. The proposed method adaptively adjusts the position of the RX-MA based simply on channel measurements, without the need of acquiring the channel response between the TX and the RX over the entire movable regions. Simulation results show that the proposed method presents a significant performance advantage over the CSI-based method when the number of channel measurements is limited.

REFERENCES

- [1] L. Zhu, W. Ma, and R. Zhang, "Movable-antenna array enhanced beamforming: Achieving full array gain with null steering," *IEEE Communications Letters*, 2023.
- [2] L. Zhu, W. Ma, and R. Zhang, "Movable antennas for wireless communication: Opportunities and challenges," *IEEE Communications Magazine*, 2023.
- [3] L. Zhu, W. Ma, and R. Zhang, "Modeling and performance analysis for movable antenna enabled wireless communications," *IEEE Transactions on Wireless Communications*, 2023.
- [4] S. Sanayei and A. Nosratinia, "Antenna selection in MIMO systems," *IEEE Communications Magazine*, vol. 42, no. 10, pp. 68–73, 2004.
- [5] M. Gharavi-Alkhanjari and A. B. Gershman, "Fast antenna subset selection in MIMO systems," *IEEE Transactions on Signal Processing*, vol. 52, no. 2, pp. 339–347, 2004.
- [6] L. Zhu, W. Ma, B. Ning, and R. Zhang, "Movable-antenna enhanced multiuser communication via antenna position optimization," *IEEE Transactions on Wireless Communications*, 2023.
- [7] Z. Xiao, X. Pi, L. Zhu, X.-G. Xia, and R. Zhang, "Multiuser communications with movable-antenna base station: Joint antenna positioning, receive combining, and power control," *arXiv preprint arXiv:2308.09512*, 2023.
- [8] B. Ning, S. Yang, Y. Wu, P. Wang, W. Mei, C. Yuen, and E. Björnson, "Movable antenna-enhanced wireless communications: General architectures and implementation methods," *arXiv preprint arXiv:2407.15448*, 2024.
- [9] Z. Xiao, S. Cao, L. Zhu, Y. Liu, B. Ning, X.-G. Xia, and R. Zhang, "Channel estimation for movable antenna communication systems: A framework based on compressed sensing," *IEEE Transactions on Wireless Communications*, 2024.
- [10] W. Ma, L. Zhu, and R. Zhang, "Compressed sensing based channel estimation for movable antenna communications," *IEEE Communications Letters*, 2023.
- [11] B. Shahriari, K. Swersky, Z. Wang, R. P. Adams, and N. De Freitas, "Taking the human out of the loop: A review of bayesian optimization," *Proceedings of the IEEE*, vol. 104, no. 1, pp. 148–175, 2015.
- [12] J. Larson, M. Menickelly, and S. M. Wild, "Derivative-free optimization methods," *Acta Numerica*, vol. 28, pp. 287–404, 2019.
- [13] A. S. Berahas, L. Cao, K. Choromanski, and K. Scheinberg, "A theoretical and empirical comparison of gradient approximations in derivative-free optimization," *Foundations of Computational Mathematics*, vol. 22, no. 2, pp. 507–560, 2022.
- [14] X. Chen, S. Liu, K. Xu, X. Li, X. Lin, M. Hong, and D. Cox, "Zoadamm: Zeroth-order adaptive momentum method for black-box optimization," *Advances in neural information processing systems*, vol. 32, 2019.
- [15] S. Liu, P.-Y. Chen, B. Kailkhura, G. Zhang, A. O. Hero III, and P. K. Varshney, "A primer on zeroth-order optimization in signal processing and machine learning: Principals, recent advances, and applications," *IEEE Signal Processing Magazine*, vol. 37, no. 5, pp. 43–54, 2020.

- [16] P.-Y. Chen, H. Zhang, Y. Sharma, J. Yi, and C.-J. Hsieh, "Zoo: Zeroth order optimization based black-box attacks to deep neural networks without training substitute models," in *Proceedings of the 10th ACM workshop on artificial intelligence and security*, 2017, pp. 15–26.